Bioresource Technology 163 (2014) 308–319

Contents lists available at ScienceDirect

Bioresource Technology

journal homepage: www.elsevier.com/locate/biortech

Influence of light absorption rate by *Nannochloropsis oculata* on triglyceride production during nitrogen starvation

Razmig Kandilian [a,b], Jérémy Pruvost [a], Jack Legrand [a], Laurent Pilon [b,*]

[a] Université de Nantes, CNRS, GEPEA, UMR-CNRS 6144, Bd de l'Université, CRTT-BP 406, 44602 Saint-Nazaire Cedex, France
[b] Mechanical and Aerospace Engineering Department, Henry Samueli School of Engineering and Applied Science, University of California – Los Angeles, Los Angeles, CA 90095, USA

HIGHLIGHTS

- Radiation properties of *N. oculata* were measured during sudden nitrogen starvation.
- Light absorption rate by *N. oculata* decreases during sudden nitrogen starvation.
- Triglyceride TG-FA productivity correlates with light absorption rate by cells.
- A critical light absorption rate should be exceeded for large TG-FA accumulation.
- Conclusions were valid for both sudden and progressive nitrogen starvation.

GRAPHICAL ABSTRACT

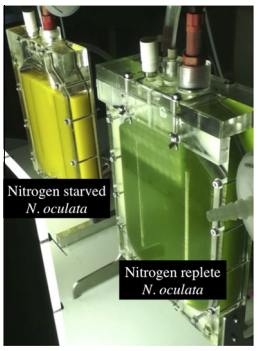

ARTICLE INFO

Article history:
Received 26 February 2014
Received in revised form 11 April 2014
Accepted 14 April 2014
Available online 24 April 2014

Keywords:
Microalgae
Biodiesel
Triglyceride lipids
Photobioreactors
bioprocess optimization

ABSTRACT

This study aims to understand the role of light transfer in triglyceride fatty-acid (TG-FA) cell content and productivity from microalgae during nitrogen starvation. Large amounts of TG-FA can be produced via nitrogen starvation of microalgae in photobioreactors exposed to intense light. First, spectral absorption and scattering cross-sections of *N. oculata* were measured at different times during nitrogen starvation. They were used to relate the mean volumetric rate of energy absorption (MVREA) per unit mass of microalgae to the TG-FA productivity and cell content. TG-FA productivity correlated with the MVREA and reached a maximum for MVREA of 13 $\mu mol_{hv}/g\,s$. This indicated that TG-FA synthesis was limited by the photon absorption rate in the PBR. A minimum MVREA of 13 $\mu mol_{hv}/g\,s$ was also necessary at the onset of nitrogen starvation to trigger large accumulation of TG-FA in cells. These results will be instrumental in defining protocols for TG-FA production in scaled-up photobioreactors.

1. Introduction

Microalgae are being considered as a renewable alternative for biodiesel production and carbon sequestration (Chisti, 2007; le B. Williams and Laurens, 2010). These single cell microorganisms have significantly larger photosynthetic efficiency than higher plants and can contain large amounts of lipids by dry weight (Ke, 2001; Chisti, 2007; le B. Williams and Laurens, 2010). Some of these lipids can then be converted into biodiesel (Chisti, 2007). Microalgae are typically grown in outdoor photobioreactors (PBRs) which can be controlled and/or optimized in terms of geometry, biomass concentration, temperature, pH, and growth media composition. However, several challenges associated with cost and productivity have to be overcome for microalgal biodiesel

* Corresponding author. Tel.: +1 (310) 206 5598.
E-mail addresses: Jeremy.Pruvost@univ-nantes.fr (J. Pruvost), pilon@seas.ucla.edu (L. Pilon).

http://dx.doi.org/10.1016/j.biortech.2014.04.045
0960-8524/

production to be financially viable (Oeschger and Posten, 2012). Among them, increasing and optimizing areal lipid productivity is essential for industrial-scale deployment of the technology (Oeschger and Posten, 2012).

Several strategies can be used to enhance lipid productivity (le B. Williams and Laurens, 2010). For example, nitrogen starvation triggers large amounts of lipid accumulation (Hu et al., 2008; Van Vooren et al., 2012). The stressful conditions of nitrogen starvation lead cells to synthesize neutral lipids mainly in the form of triglyceride fatty acids (TG-FA) (Van Vooren et al., 2012). They are believed to serve as carbon and energy storage compound for the cells (Hu et al., 2008). TG-FA are the main feedstock for lipid to biodiesel conversion through transesterification reaction with methanol to produce methyl esters of fatty acids that are essentially biodiesel (Chisti, 2007). The accumulation of TG-FA during nitrogen starvation has been observed in numerous microalgal species including *Nannochloropsis oculata* (Van Vooren et al., 2012), *Nannochloropsis* sp. (Pal et al., 2011), *Neochloris oleoabundans* (Pruvost et al., 2009), *Scenedesmus obliquus* (Breuer et al., 2013), *Chlorella* sp., and many others (Adams et al., 2013). Typically, 40–50 dry wt.% is the maximum concentration of TG-FA reported in microalgae cells (Hu et al., 2008). In addition, subjecting the cells to intense light during nitrogen starvation has been shown to be essential in TG-FA synthesis (Hu et al., 2008; Van Vooren et al., 2012). This is in contrast to the synthesis and accumulation of polar lipids under light limited growth conditions (Hu et al., 2008). On the other hand, Breuer et al. (2013) demonstrated that TG-FA accumulation in *Scenedesmus obliquus* was independent of photon flux density (PFD) in batch grown cultures.

One of the consequences of nitrogen starvation is the reduction in the total pigment concentration in the cells as well as the increase in carotenoid to chlorophyll *a* (chl*a*) concentration ratio (Heath et al., 1990). Pruvost et al. (2009) observed a ten fold decrease in total pigment concentration in *Neochloris oleoabundans* cells during nitrogen starvation. In addition, changes in chl*a* to carotenoid ratio greatly modifies the color and light absorption of microorganisms thus affecting their ability to perform photosynthesis and accumulate TG-FA (Van Vooren et al., 2012).

The present study aims to determine the relation between light absorption rate and TG-FA cell concentration and production rate by marine microalgae *Nannochloropsis oculata*. The results will be instrumental in optimizing and defining protocols for TG-FA production in scaled up PBRs.

2. Background

2.1. Nannochloropsis oculata

In the present study, the marine eustigmatophyceae *Nannochloropsis oculata* was selected for its relatively large biomass growth rate and because it can contain large amounts of TG-FA (Van Vooren et al., 2012). It can be cultivated in seawater, thus eliminating competition with freshwater used for human consumption. Kandilian et al. (2013) recently reported the radiation characteristics and optical properties of *N. oculata* in batch grown cultures over the photosynthetically active radiation (PAR) region. A significant decrease in the absorption cross-section of the cells at wavelengths between 400 and 750 nm was observed during nitrogen limitation compared with cells grown in nitrogen replete media (Kandilian et al., 2013). Furthermore, Flynn et al. (1993) demonstrated that nitrogen deprived *N. oculata* cells can undergo two cell divisions after the onset of NH_4^+ deprivation. To do so, each cell divides its nitrogen content between the daughter cells (Flynn et al., 1993). In fact, the authors reported that nitrogen replete *N. oculata* cells had a carbon to nitrogen ratio (C/N) of 6 while NH_4^+ deprived cells featured C/N ratio of nearly 26 (Flynn et al., 1993).

Nitrogen starvation of *N. oculata* cultures can be achieved by two methods. *Sudden starvation* consists of two steps: first, microalgae are grown in nitrogen replete conditions. Then, they are transferred into a nitrogen-free medium. *Progressive starvation* consists of initially adding a small amount of nitrogen to the culture medium in the form of nitrate, for example. After inoculating the PBR, the microalgae grow and multiply until they consume all the nitrates in the medium and the culture medium becomes deprived of nitrogen. Cells subjected to progressive nitrogen starvation have a slightly different behavior than those in sudden starvation (Van Vooren et al., 2012). Indeed, the culture goes through a nitrogen replete phase followed by nitrogen limitation phase and finally a nitrogen starvation phase. By contrast, in sudden starvation, the cells go from a nitrogen replete phase directly to a nitrogen starvation phase. Nitrogen limitation results in a decrease in pigment concentrations. Therefore, cells undergoing progressive starvation enter the nitrogen starvation phase with significantly lower pigment concentrations than those subjected to sudden starvation. This modifies the light availability in the PBR in a non-obvious way. Finally, both methods can lead to appreciable amount of TG-FA accumulation (Van Vooren et al., 2012). However, in practice, progressive starvation is preferable for mass production as it requires only one production stage and does not require the costly biomass filteration/separation from growth medium and re-suspension in a nitrogen-free medium (Van Vooren et al., 2012; Oeschger and Posten, 2012).

2.2. Effect of light on N. oculata TG-FA productivity

Van Vooren et al. (2012) demonstrated that greater light availability in flat-plate PBRs used to cultivate *N. oculata* in nitrogen starvation resulted in larger lipid productivity. Indeed, peak areal TG-FA productivity was 3.6 g/m^2 day for sudden starvation of batch culture with initial biomass concentration of 0.41 kg/m^3 exposed to 250 $\mu mol_{hv}/m^2$ s compared with 1.4 g/m^2 day for the same illumination conditions when the initial biomass concentration was 0.76 kg/m^3. The larger initial biomass concentration resulted in stronger light attenuation and lower light availability in the PBR. Similarly, *N. oculata* cultivated in a 5 cm flat-plate PBR had 50% lower TG-FA productivity than those cultivated in 3 cm flat-plate PBR under the same conditions. Pal et al. (2011) also showed that nitrogen starved *Nannochloropsis* sp. grown in cylindrical PBR 6 cm in diameter and exposed to 750 $\mu mol_{hv}/m^2$ s of white light contained 35% total lipids by dry weight compared with 22% for cells grown exposed to 170 $\mu mol_{hv}/m^2$ s.

These studies established the existence of a relationship between the light attenuation conditions in the PBR and lipid or TG-FA accumulation in the cells. In order to examine this link further, it is necessary to perform light transfer analysis in the PBR and relate it to the kinetics of lipid accumulation in the cells. To do so, the radiation characteristics of the microalgae as a function of time are necessary during nitrogen starvation (Pilon et al., 2011). Because the cells undergo large changes in pigment concentrations and composition, theoretical predictions could be difficult to obtain and may be inaccurate (Berberoğlu et al., 2007). Therefore, experimental measurements were preferred in this study.

2.3. Light transfer modeling in PBRs

In photochemical reactions, the reaction kinetics are proportional to the absorbed useful energy or the specific local volumetric rate of energy absorption, $\mathscr{A}$ expressed in $\mu mol_{hv}/g\ s$ (Cassano et al., 1995). In the context of photobioreactors, it represents the amount of photons absorbed per unit time and per unit weight of biomass. In the case of photosynthetic microalgae, the useful energy is contained in the PAR region defined by the spectral

region between 400 and 700 nm. Therefore, the specific local volumetric rate of energy absorption depends on the absorption cross-section of the species and on the radiation field inside the PBR in the PAR region as recently shown by Pruvost and Cornet (2012). The authors developed a model predicting the maximum biomass productivity of both microalgae (Takache et al., 2010) and cyanobacteria (Cornet and Dussap, 2009) in various PBRs as a function of PFD. The authors used the specific mean volumetric rate of energy absorption (MVREA) denoted by $\langle \mathscr{A} \rangle$ and the photosynthesis half saturation constant of the microorganism to obtain an analytic expression for the biomass productivity (Pruvost and Cornet, 2012). The MVREA $\langle \mathscr{A} \rangle$ can be expressed as (Pruvost and Cornet, 2012)

$$\langle \mathscr{A} \rangle = \frac{1}{L} \int_{400}^{700} \int_{0}^{L} \bar{A}_{abs,\lambda} G_{\lambda}(z) dz d\lambda \tag{1}$$

where $\bar{A}_{abs,\lambda}$ is the average spectral mass absorption cross-section of the microalgae (in m^2/kg), $G_{\lambda}(z)$ is the local fluence rate in $\mu mol_{hv}/m^2$ s, and L is the thickness of the PBR (in m). The MVREA $\langle \mathscr{A} \rangle$ accounts for the cumulative effects of (i) biomass concentration, (ii) absorption cross-section of the microalgae, and (iii) the fluence rate inside the PBR. Note that all these parameters vary during the course of nitrogen starvation experiments. Therefore, $\langle \mathscr{A} \rangle$ is more indicative of the amount of light absorbed by the microalgae than the fluence rate in the PBR or the absorption cross-section of the cells considered separately.

In the case of absorbing and scattering media such as microalgal culture, the local spectral fluence rate $G_{\lambda}(z)$ can be obtained by solving the radiative transfer equation (Jonasz and Fournier, 2007). Several methods of solution exist (Pilon et al., 2011; Dauchet et al., 2013; Lee et al., 2014). However, for one-dimensional flat-plate PBRs with transparent front window containing strongly forward scattering microalgae, the two-flux approximation yields satisfactory results (Pottier et al., 2005; Lee et al., 2014). In the case of normally incident radiation $G_{\lambda,0}$, the local fluence rate $G_{\lambda}(z)$ at depth z can be expressed as

$$\frac{G_{\lambda}(z)}{G_{\lambda,0}} = 2\frac{[\rho_{\lambda}(1+\alpha_{\lambda})e^{-\delta_{\lambda}L} - (1-\alpha_{\lambda})e^{-\delta_{\lambda}L}]e^{\delta_{\lambda}z} + [(1+\alpha_{\lambda})e^{\delta_{\lambda}L} - \rho_{\lambda}(1-\alpha_{\lambda})e^{\delta_{\lambda}L}]e^{-\delta_{\lambda}z}}{(1+\alpha_{\lambda})^2 e^{\delta_{\lambda}L} - (1-\alpha_{\lambda})^2 e^{-\delta_{\lambda}L} - \rho_{\lambda}(1-\alpha_{\lambda}^2)e^{\delta_{\lambda}L} + \rho_{\lambda}(1-\alpha_{\lambda}^2)e^{-\delta_{\lambda}L}} \tag{2}$$

where ρ_{λ} is the diffuse reflectance of the PBR's back wall while the coefficients α_{λ} and δ_{λ} are expressed as (Pottier et al., 2005)

$$\alpha_{\lambda} = \sqrt{\frac{\bar{A}_{abs,\lambda}}{\bar{A}_{abs,\lambda} + 2b_{\lambda}\bar{S}_{sca,\lambda}}} \quad \text{and} \quad \delta_{\lambda} = X\sqrt{\bar{A}_{abs,\lambda}(\bar{A}_{abs,\lambda} + 2b_{\lambda}\bar{S}_{sca,\lambda})} \tag{3}$$

Here, $\bar{S}_{sca,\lambda}$ (in m^2/kg) is the average spectral mass scattering cross-section of the microalgae suspension. The biomass concentration is denoted by X and expressed in kg of dry weight per m^3 of suspension. The backward scattering ratio b_{λ} is defined as the fraction of the radiation scattered backwards and is estimated from the suspension's scattering phase function (Pottier et al., 2005). It is approximately constant over the PAR region and was recently measured to be 0.002 for *N. oculata* (Kandilian et al., 2013). The PAR-averaged fluence rate $G_{PAR}(z)$ can be expressed as

$$G_{PAR}(z) = \int_{400}^{700} G_{\lambda}(z) dz. \tag{4}$$

Note that in batch cultivation, absorption and scattering cross-sections of the microalgae as well as the biomass concentration are all time-dependent.

Finally, the areal TG-FA productivity R (in g/m^2 day) of a culture can be expressed as

$$R(t) = L\frac{d[\mathrm{TG-FA}](t)}{dt} \tag{5}$$

where $[\mathrm{TG\text{-}FA}](t)$ (in kg/m^3) corresponds to the culture's TG-FA concentration at time t. In practice, with daily sampling of the culture, the areal daily average TG-FA productivity $\bar{R}$ of a batch culture can be written as

$$\bar{R}(t_i) = L\frac{[\mathrm{TG-FA}](t_i) - [\mathrm{TG-FA}](t_{i-1})}{(t_i - t_{i-1})} \tag{6}$$

where t_i and t_{i-1} correspond to two consecutive sampling times 24 h apart.

2.4. Determination of radiation characteristics

2.4.1. Experimental determination

The average spectral mass absorption and scattering cross-sections $\bar{A}_{abs,\lambda}$ and $\bar{S}_{sca,\lambda}$ can be experimentally measured according to a procedure reviewed by Pilon et al. (2011). In this method, the normal-normal and normal-hemispherical transmissions of several dilute microalgae suspensions with different known concentrations are measured using a spectrometer equipped with an integrating sphere. First, the apparent extinction coefficient χ_{λ} can be obtained from normal-normal transmittance $T_{n,\lambda}$ measurements of cuvettes, of pathlength t, filled with microalgae suspension $T_{n,\lambda,X}$ or with the reference medium $T_{n,\lambda,ref}$

$$\chi_{\lambda} = -\frac{1}{t} ln\left(\frac{T_{n,\lambda,X}}{T_{n,\lambda,ref}}\right) \tag{7}$$

Similarly, the apparent absorption coefficient $\chi_{h,\lambda}$ can be defined from the hemispherical transmittance $T_{h,\lambda}$ by

$$\chi_{h,\lambda} = -\frac{1}{t} ln\left(\frac{T_{h,\lambda,X}}{T_{h,\lambda,ref}}\right) \tag{8}$$

The apparent extinction coefficient χ_{λ} can be expressed as a function of the actual absorption κ_{λ} and scattering $\sigma_{s,\lambda}$ coefficients

$$\chi_{\lambda} = \kappa_{\lambda} + (1-\epsilon_n)\sigma_{s,\lambda}. \tag{9}$$

Here, ϵ_n represents the fraction of light scattered in the forward direction and detected by the spectrometer. Ideally, ϵ_n is equal to unity. However, due to the finite size of the acceptance angle of the detector, ϵ_n is typically smaller than 1 and is assumed to be constant over the PAR region. It is estimated from microorganism scattering phase function $\Phi_{\lambda}(\Theta)$ as follows

$$\epsilon_n = \frac{1}{2}\int_{0}^{\Theta_a} \Phi_{\lambda}(\Theta)\sin\Theta d\Theta \tag{10}$$

where Θ_a is the half acceptance angle of the detector. The actual extinction coefficient $\beta_{\lambda} = \kappa_{\lambda} + \sigma_{s,\lambda}$ can then be determined according to

$$\beta_{\lambda} = \frac{\chi_{\lambda} - \epsilon_n\kappa_{\lambda}}{1-\epsilon_n} \tag{11}$$

Similarly, the apparent absorption coefficient $\chi_{h,\lambda}$ can be related to the real absorption κ_{λ} and scattering $\sigma_{s,\lambda}$ coefficients as

$$\chi_{h,\lambda} = \kappa_{\lambda} + (1-\epsilon_h)\sigma_{s,\lambda} \tag{12}$$

Here, ϵ_h is the fraction of the scattered light detected by the detector. Ideally, when all the scattered light is accounted for, ϵ_h is equal to unity. Moreover, at $\lambda = 750$ nm the microorganisms are assumed to be non-absorbing, i.e., $\kappa_{750} = 0\ m^{-1}$. Then, Eqs. (9) and (12) at 750 nm simplify to

$$\chi_{h,750} = (1-\epsilon_h)\sigma_{s,750} \quad \text{and} \quad \chi_{750} = (1-\epsilon_n)\sigma_{s,750} \tag{13}$$

Combining Eqs. (11)–(13) yields

$$\kappa_\lambda = \chi_{h,\lambda} - \chi_{h,750}\frac{\chi_\lambda - \chi_{h,\lambda}}{\chi_{750} - \chi_{h,750}} \quad \text{and} \quad \sigma_{s,\lambda} = \frac{\chi_\lambda - \epsilon_n\kappa_\lambda}{1-\epsilon_n} - \kappa_\lambda \tag{14}$$

Finally, the average mass absorption $\bar{A}_{abs,\lambda}$ and scattering $\bar{S}_{sca,\lambda}$ cross-sections of the microalgae are defined as

$$\bar{A}_{abs,\lambda} = \kappa_\lambda / X \quad \text{and} \quad \bar{S}_{sca,\lambda} = \sigma_{s,\lambda}/X \tag{15}$$

2.4.2. Semi-empirical determination

Alternatively, the average mass absorption cross-section $\bar{A}_{abs,\lambda}$ of a phytoplanktonic suspension can be estimated as a weighted sum of the effective mass absorption cross-sections $a^*_{i,\lambda}$ of pigment i present in the microalgae cells (Bidigare et al., 1990; Nelson et al., 1993; Bricaud et al., 2004)

$$\bar{A}_{abs,\lambda} = \sum_{i=1}^{n} C_i a^*_{i,\lambda} + \omega_\lambda \tag{16}$$

Here, C_i is the concentration of pigment i and ω_λ is a semi-empirical function independent of any pigment concentration (Nelson et al., 1993; Bricaud et al., 2004). This average mass absorption cross-section takes into account the package effect responsible for a decrease in the effective absorption cross-section of the pigments once they are packaged into the cells (Nelson et al., 1993; Bricaud et al., 2004). It can be estimated by considering the ratio of the *in vivo* and *ex vivo* absorption cross-sections of the cell's pigments (Bricaud et al., 2004). Bricaud et al. (2004) and Nelson et al. (1993) measured the absorption cross-section $\bar{A}_{abs,\lambda}$ of various microalgae cells as well as the cells' pigment concentrations using high precision liquid chromatography (HPLC). The authors then compared the measured absorption cross-section $\bar{A}_{abs,\lambda}$ to that predicted by Eq. (16) accounting for 20 different pigments. To minimize the error between the predicted and measured average spectral absorption cross-sections $\bar{A}_{abs,\lambda}$, both studies reported the necessity to introduce the term ω_λ in Eq. (16) (Nelson et al., 1993; Bricaud et al., 2004). However, there is no clear consensus in the literature on the origin of this term. It has been attributed to (i) intracellular pigments that cannot be extracted by solvents such as methanol or acetone (Bricaud et al., 2004) and (ii) to absorption by the cell walls and cytoplasm that are filtered out during pigment extraction (Bissett et al., 1997; Bricaud et al., 2004).

2.4.3. Theoretical predictions

Theoretical predictions of $\bar{A}_{abs,\lambda}$ and $\bar{S}_{sca,\lambda}$ can be obtained by Lorenz-Mie theory based on the cell size distribution and on the effective complex index of refraction of the microalgae on spectral basis over the PAR region (Pottier et al., 2005; Berberoğlu et al., 2007; Jonasz and Fournier, 2007). Flynn et al. (1993) observed a 30% increase in the volume of *N. oculata* cells during NH_4^+ starvation. Unfortunately, changes in the real part of the complex index of refraction due to nitrogen starvation have not been reported in the literature. However, it is a function of the cell's composition including lipid, protein, and carbohydrates mass fractions (Jonasz and Fournier, 2007). Thus, a large increase in cell lipid content would lead to changes in the cell's effective refraction index and therefore in its average spectral scattering cross-section. Therefore, experimentally measuring the absorption and scattering cross-sections appeared to provide a more reliable and accurate method of accounting for changes in composition and cell size distribution during nitrogen starvation.

3. Materials and methods

3.1. Species and culture medium

A strain of *Nannochloropsis oculata* was obtained from Alphabiotech collection (Asserac, France). The microalgae were cultivated in a modified Conway medium using an artificial seawater (ASW) base (Berges et al., 2001) with salinity of 25 g/L. The Conway medium composition was (in mM): $Na_2EDTA\cdot 2H_2O$, 0.36; H_3BO_3, 1.63; NaH_2PO_4, 1.50; $FeCl_3\cdot 6H_2O$, 0.01; $MnCl_2\cdot 4H_2O$, 0.91; $ZnCl_2$, 0.023; $CoCl_2\cdot 6H_2O$, 0.013; $CuSO_4\cdot 5H_2O$, 0.012; $Na_2MoO_4\cdot 5H_2O$, 0.008. The medium was filter-sterilized using 0.22 µm liquid filter (AcroPak 20, Pall Corp., Port Washington, NY).

Sudden starvation experiments were performed by inoculating the PBRs with *N. oculata* produced by a continuous PBR illuminated with 150 $\mu mol_{hv}/m^2$ s. A specific volume of culture was harvested and centrifuged at 10,000*g* (ThermoScientific Sorvall RC 6 Plus, Massachusetts, USA) for 5 min at 4 °C, washed with nitrogen-free Conway medium and injected into the PBR filled with the nitrogen-free medium. The volume of culture was chosen based on the desired initial biomass concentration of the nitrogen starvation batch.

3.2. Photobioreactor

The nitrogen starvation experiments were performed in batch mode in a 1 L airlift-type flat-panel PBR with thickness of 3 cm. The PBR was described in more detail by Pruvost et al. (2009). Illumination was provided on one face of the PBR by a white LED light panel (P4 Cool White, Seoul Semiconductor) with adjustable PFD. The illuminated surface of the PBR was made of transparent polymethyl methacrylate (PMMA) and the backwall of diffuse stainless steel with diffuse reflectance ρ_λ of 0.2 over the PAR region (Takache et al., 2010). The incident PFD was measured over the PAR region at 12 different locations on the inside surface of the PBR using a quantum light sensor (Li-250A, Li-COR, Lincoln, NE). The measured PFD varied by less than 10% for the different locations measured the average PFDs was reported. The pH was continuously measured using a pH sensor (Mettler Toledo SG 3253) and was maintained at 8 by automatic CO_2 injection when the culture pH exceeded 8. Mixing in the PBR was provided by injecting air at a flow rate of 80 mL/min. The PBR was maintained at room temperature (approximately 22.5 °C) by forced air convection on the back of the PBR. Before starting each experiment, the PBR was sterilized for 30 min using a 5 mM peroxyacetic acid solution and rinsed twice with sterile deionized water.

3.3. Biomass concentration

Microorganisms dry biomass concentration X was determined gravimetrically by filtering 5 mL of culture through a pre-dried and pre-weighed 0.45 µm pore size glass-fiber filter (Whatman GF/F). The filters were dried overnight in an oven at 105 °C and weighed after being cooled in a desiccator for 20 min. The samples were analyzed in triplicates and the reported biomass concentration corresponded to the mean value.

3.4. Pigment concentration

Pigments were extracted in pure methanol and quantified spectrophotometrically. A volume of 0.5 mL of culture was first centrifuged at 13,400 rpm (12,100*g*) for 15 min. The medium was discarded and the cells were resuspended in 1.25 mL pure methanol and sonnicated for 10 s. Pigments were extracted for a period of 1 h at 45 °C and the extract was centrifuged. The

optical density OD_{λ} of the supernatant was measured at wavelengths 750, 665, 652, and 480 nm using a UV–vis–NIR spectrophotometer (Agilent Cary 5000, Santa Clara, CA). All extractions were performed in triplicates. Chlorophyll *a* concentration, denoted by C_{chla}, was estimated according to the correlation (Ritchie, 2006)

$$C_{chla}[mg/L] = -8.0962(OD_{652} - OD_{750}) + 16.5169(OD_{665} - OD_{750}) \quad (17)$$

Similarly, photo-protective carotenoid (PPC) concentration C_{PPC} was estimated according to (Strickland and Parsons, 1968)

$$C_{PPC}[mg/L] = 4(OD_{480} - OD_{750}) \quad (18)$$

3.5. Radiation characteristics

The radiation characteristics of the microalgae were measured experimentally using the method reviewed by Pilon et al. (2011). The normal-normal transmission measurements were performed using a UV–vis–NIR spectrophotometer (Agilent Cary 5000, Santa Clara, CA). The normal-hemispherical transmission measurements were performed using an integrating sphere attachment (Agilent Cary DRA-2500, Santa Clara, CA) to the aforementioned spectrophotometer. The experimental setup and procedure and the data analysis were successfully validated by comparing the measured scattering cross-sections of polystyrene spheres 2.02 and 4.5 μm in diameter to those predicted by Lorenz–Mie theory according to the analysis presented by Berberoğlu et al. (2008) (see Supplementary Material). To avoid absorption and scattering by the growth medium, the microalgae were centrifuged at 13,400 rpm for 20 min and washed twice with phosphate buffer saline (PBS) solution and suspended in PBS. The measurements were performed in 1 cm pathlength quartz cuvettes (110–10-40 Hellma Analytics, Müllheim, Germany) in the wavelength range from 350 to 750 nm. The microalgae suspensions were diluted to ensure that single scattering prevailed. The average mass absorption and mass scattering cross-sections of microalgae suspensions were measured for three biomass concentrations between 0.03 and 0.10 kg/m^3 to ensure that they were independent of microalgae concentration *X*. The cross-sections reported correspond to the mean of the three measurements.

3.6. Lipid extraction

Lipid extraction was performed according to the whole cell analytic method outlined by Van Vooren et al. (2012). Briefly, 2 mL of culture were centrifuged for 10 min at 3600 *g* and the supernatant was discarded. The cells were then resuspended in chloroform/methanol mixture (2:1 by volume) and sonicated for 30 s followed by 6 h of light agitation on a tube roller. The extracts were dried under pure nitrogen and recovered with 1 mL of chloroform/methanol mixture (2:1 by volume). Triglyceride lipids were separated from the other lipids by solid phase extraction. Finally, the lipids were transesterified and their concentration was measured by gas chromatography with a flame ionization detector (ThermoFisher).

4. Results

Three sudden starvation experiments were performed with different initial biomass concentrations X_0. In all cases, the front face of the PBR was exposed to an incident PFD of 250 $\mu mol_{hv}/m^2$ s.

4.1. Biomass concentration

Fig. 1a shows the temporal evolution of the biomass concentration of *N. oculata* grown in batch mode and subjected to sudden nitrogen starvation with initial biomass concentrations X_0 of 0.23, 0.41, and 0.85 kg/m^3. It indicates that the biomass concentration increased nearly linearly with time in the nitrogen-free medium. Cells were able to divide despite the absence of nitrogen as previously demonstrated and discussed by Flynn et al. (1993). Note that nitrogen starved *N. oculata* cells featured approximately one to two orders of magnitude smaller biomass productivity than those cultivated in nitrogen replete media. The three batches reached biomass concentrations of 0.84, 1.3, and 2.18 kg/m^3 after 96 h of cultivation, respectively. For comparison purposes, biomass concentrations reported by Van Vooren et al. (2012) for experiments with initial concentration X_0 equal to 0.23 and 0.41 kg/m^3 were added to Fig. 1. The values obtained in the present study agreed with those reported by Van Vooren et al. (2012) for identical growth conditions. This confirms the repeatability of the measurements. The present study provides additional and more detailed information on the temporal evolution of *N. oculata* during nitrogen starvation.

4.2. Pigment concentrations

Fig. 1b and c show the temporal evolution of chl*a* and carotenoid concentrations during sudden starvation cultivation for the three different initial biomass concentrations X_0 considered. They indicate that the cell pigment concentration decreased immediately after the microalgae were suspended in the nitrogen-free medium. Most of this decrease occurred within the first 24 h. Here also, the pigment concentrations were similar to those reported by Van Vooren et al. (2012). Moreover, it is apparent that the rate of pigment loss was correlated with the initial biomass concentration. In fact, after 96 h of cultivation, the chl*a* concentration C_{chla} in culture with $X_0 = 0.23$ kg/m^3 was 0.23 wt.% compared with 0.31 and 0.59 wt.% for cells cultivated in the same PBR with initial concentration X_0 of 0.41 and 0.85 kg/m^3, respectively. This was due to the fact that batches with smaller initial biomass concentration had larger cell growth rates. This resulted in faster decrease of cell nitrogen content thus increasing the rate of chl*a* loss in cells. Indeed, by 96 h, the biomass concentration had grown by 3.6 times for the batch with initial concentration X_0 of 0.23 kg/m^3 while it had increased by only 3.1 and 2.4 times for batches with X_0 equal to 0.41 and 0.85 kg/m^3, respectively. These corresponded to a time-averaged growth rates of 27.6×10^{-3}, 22.6×10^{-3}, and 16.2×10^{-3} h^{-1}, respectively.

4.3. Stress index

The stress index is defined as the ratio of the optical densities (OD) of the cells' pigment extract at wavelengths 480 and 665 nm (Heath et al., 1990). It is an indicator of the "nutrient status" of the cells as proposed by Heath et al. (1990). It is an indirect measure of the carotenoid to chl*a* ratio and it is inversely correlated to the C/N ratio of the cells (Heath et al., 1990). Fig. 1d shows the stress index for the three batch cultivations previously described. In nutrient replete conditions, corresponding to cultivation time t =0, the stress index was approximately 0.5. For all sudden starvation experiments it increased with time and was larger for cultures with smaller initial biomass concentration X_0. In fact, the stress index after 96 h of cultivation was 1.8, 1.5, and 0.9 for cultures with initial biomass concentration X_0 of 0.23, 0.41 and 0.85 kg/m^3, respectively. This indicates that cells in the culture with initial concentration $X_0 = 0.23$ kg/m^3 had undergone more cell divisions and thus featured a larger C/N ratio.

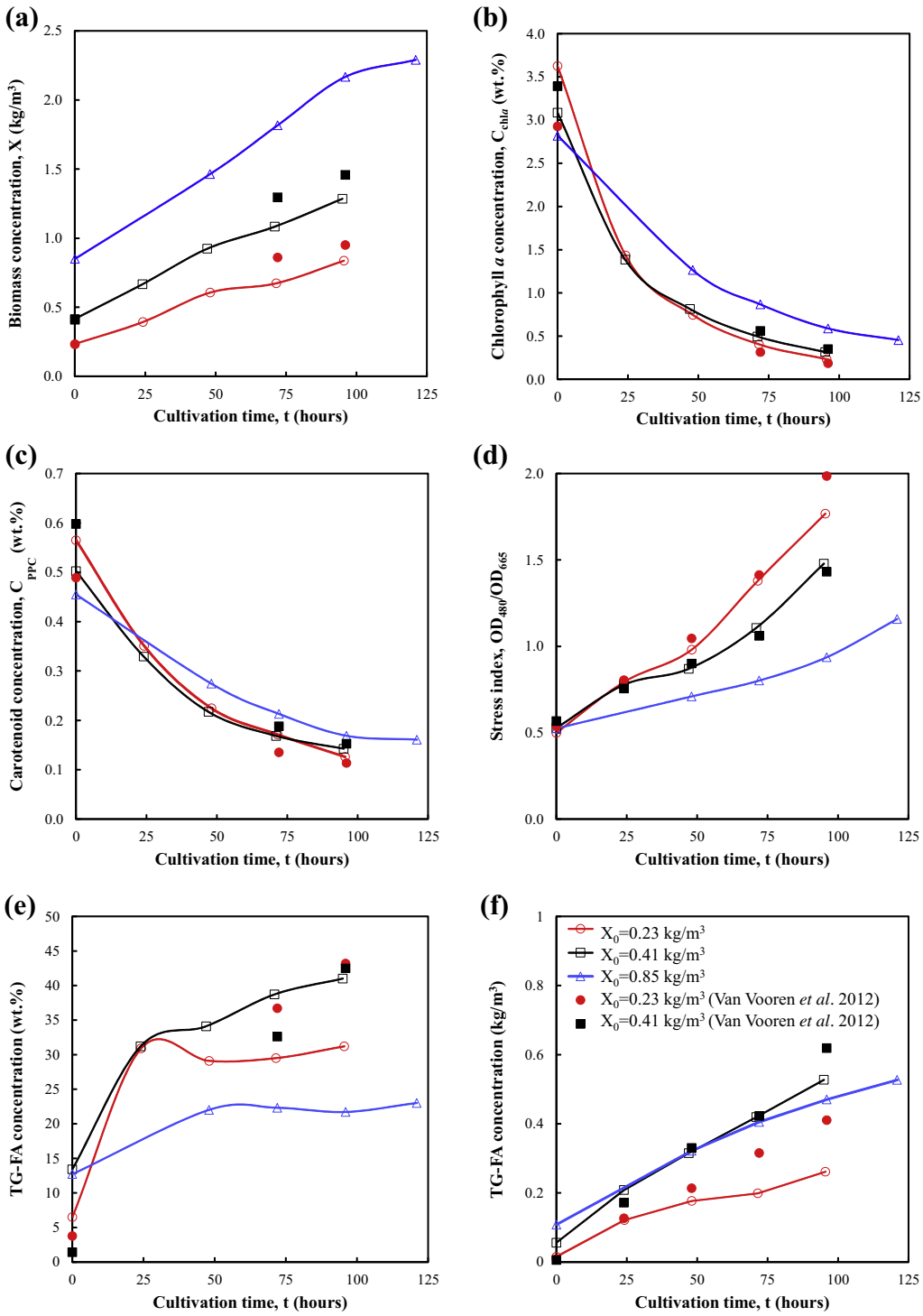

Fig. 1. Temporal evolution of (a) biomass concentration X, (b) chlorophyll *a* concentration C_{chla}, (c) carotenoid concentration C_{PPC}, (d) the stress index, (e) TG-FA concentration (dry wt.%), and (f) TG-FA concentration (kg/m^3) during sudden nitrogen starvation of batch culture exposed to 250 µmol$_{hv}$/m^2 s with initial biomass concentrations X_0 equal to 0.23, 0.41, and 0.85 kg/m^3. Data reported by Van Vooren et al. (2012) for experiments with initial concentration X_0 = 0.23 and 0.41 kg/m^3 were added for reference.

4.4. TG-FA concentration

Fig. 1e and f show the temporal evolution of the TG-FA concentration in dry wt.% and in kg/m^3, respectively, for *N. oculata* grown in batch mode and subjected to sudden nitrogen starvation with initial biomass concentrations X_0 of 0.23, 0.41, and 0.85 kg/m^3. It indicates an immediate increase in TG-FA concentration in cells following their suspension in nitrogen-free medium. Indeed, experiments with initial concentration X_0 of 0.23, 0.41, and 0.85 kg/m^3 featured cells that reached a TG-FA concentration of 30, 31, and 21 dry wt.% after 24 h, respectively. The culture with initial concentration X_0 equal to 0.41 kg/m^3 reached a final TG-FA concentration of 41.2 dry wt.%. This compared well with the TG-FA concentration of 42 dry wt.% reported by Van Vooren et al. (2012) for an identical experiment. On the other hand Van Vooren et al. (2012) reported a final TG-FA concentration of 43%

for sudden starvation experiment with initial biomass concentration X_0 of 0.23 k/m^3. This was significantly different from the 30 dry wt.% obtained here. In addition, it is unusual to observe a decrease in the TG-FA concentration such as that seen after 48 h of cultivation in continuously illuminated cultures. This may be attributed to experimental uncertainties in the lipid extraction or analysis. Note, however, that other measurements (Fig. 1a–d) were consistent with data reported by Van Vooren et al. (2012).

4.5. Radiation characteristics

Fig. 2a and b show the temporal evolution of the measured average mass absorption and scattering cross-sections in the spectral region from 350 to 750 nm for *N. oculata* during sudden nitrogen starvation of the batch culture with an initial biomass concentration X_0 of 0.23 kg/m^3. Overall, the mass absorption cross-section decreased as a function of time for all wavelengths in the PAR region. Similar results were obtained for experiments with different initial biomass concentrations (see Supplementary materials). The decrease in absorption cross-section was consistent with the continuous decrease in pigment concentrations over time observed in Fig. 1b and c. For example, the chl*a* absorption peak at 676 nm decreased from 544 m^2/kg at the start of cultivation to only 43 m^2/kg after 96 h for the culture with initial concentration $X_0 = 0.23$ kg/m^3. During the same time period, the chl*a* concentration decreased from 3.6 wt.% to 0.23 wt.%. Such sharp decrease in the mass absorption cross-section had a significant effect on the PAR-averaged fluence rate $G_{PAR}(z)$ in the PBR.

Moreover, the magnitude and shape of the average mass scattering cross-section changed slightly over time. For example, it decreased by 20% at 555 nm corresponding to the lowest absorption cross-section. However, it increased by 5.5% at wavelength 437 nm corresponding to one of chlorophyll *a* absorption peaks. Changes in the scattering cross-section overtime could be due to changes in size, shape, cellular composition, and pigment concentrations of the cells (Jonasz and Fournier, 2007). However, it is difficult to attribute the observed changes specifically to any one or more of those parameters due to the complexity of the biological response to nitrogen starvation (Flynn et al., 1993).

In the present study, the concentrations of chlorophyll *a* C_{chla} and the photo-protective carotenoids C_{PPC} were measured. Then Eq. (16) can be written as

$$\bar{A}_{abs,\lambda} = a^*_{chla,\lambda} C_{chla} + a^*_{PPC,\lambda} C_{PPC} + \omega_\lambda \tag{19}$$

Here, $a^*_{chla,\lambda}$ and $a^*_{PPC,\lambda}$ (in m^2/kg) correspond to the effective specific absorption cross-sections of chl*a* and PPC, respectively. Fig. 2c presents the coefficients $a^*_{chla,\lambda}$, $a^*_{PPC,\lambda}$, and ω_λ obtained by fitting 15 experimentally measured spectral mass absorption cross-sections

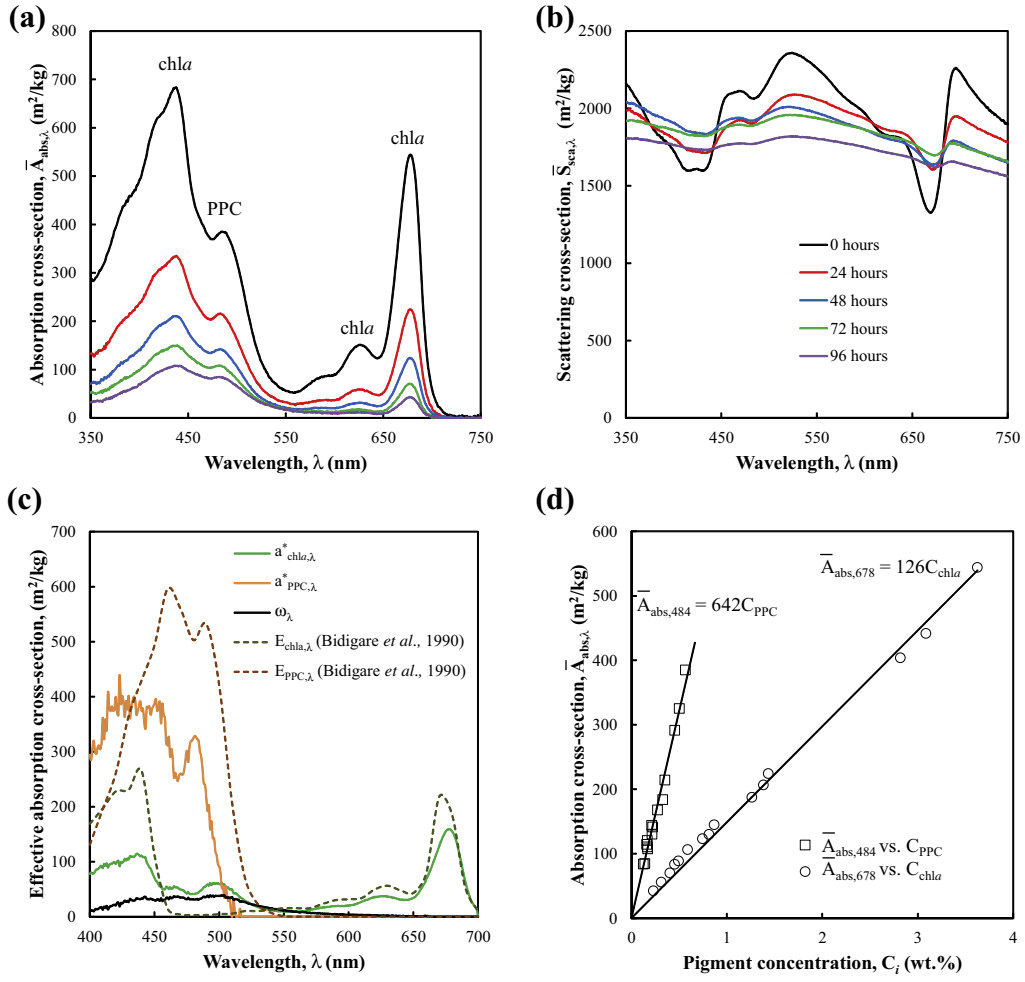

Fig. 2. Average mass (a) absorption and (b) scattering cross-sections of *N. oculata* after 0, 24, 48, 72, and 96 h of cultivation during sudden nitrogen starvation of batch culture exposed to 250 $\mu mol_{hv}/m^2$ s with an initial biomass concentration $X_0 = 0.23$ kg/m^3. (c) Retrieved pigment effective absorption cross-sections $a^*_{chla,\lambda}$, $a^*_{PPC,\lambda}$, and coefficient ω_λ used in Eq. (19). (d) Absorption cross-section at 676 nm $\bar{A}_{abs,676}$ as a function of chl*a* concentration C_{chla} and absorption cross-section at 484 nm $\bar{A}_{abs,484}$ as a function of carotenoid concentration C_{PPC} compiled from all three experiments.

to Eq. (19) using the least squares method. It also shows the *ex-vivo* absorption cross-sections of chl*a*, $Ea_{chla,\lambda}$, and PPC, $Ea_{PPC,\lambda}$, (in m^2/kg) reported by Bidigare et al. (1990). The retrieved pigment effective absorption cross-sections $a^*_{chla,\lambda}$ and $a^*_{PPC,\lambda}$ show similar trends but were smaller than those reported by Bidigare et al. (1990). The differences can be attributed to the package effect and was indirectly accounted for by $a^*_{i,\lambda}$ and ω_λ. Note that during nitrogen starvation the specific types of carotenoid pigments in the cells change shifting the wavelength and the magnitude of their absorption peaks (Cohen, 1999). However, this cannot be accounted for with spectrophotometric pigment measurements. Consequently, the absorption cross-section of carotenoids $a^*_{PPC,\lambda}$ should be considered as a mean cross-section for the various carotenoids produced by *N. oculata* during nitrogen starvation. Fig. 2d show the measured average mass absorption cross-sections $\bar{A}_{abs,676}$ and $\bar{A}_{abs,484}$ at wavelengths 676 and 484 nm versus the simultaneously measured chl*a* and PPC concentrations C_{chla} and C_{PPC}, respectively. Linear relationships were found between $\bar{A}_{abs,676}$ and C_{chla} and between $\bar{A}_{abs,484}$ and C_{PPC} with coefficient of determination R^2 exceeding 0.98. This provided confidence in the accuracy and the consistency of the measured radiation characteristics as well as the measured pigment concentrations for the different experiments.

4.6. Fluence rate and MVREA

Fig. 3a shows the PAR-averaged fluence rate $G_{PAR}(z)$ predicted by Eqs. (2)–(4) as a function of PBR depth z using the radiation characteristics measured after 0 and 96 h during sudden starvation experiments with initial biomass concentration X_0 of 0.23, 0.41, and 0.85 kg/m^3. As expected, the fluence rate $G_{PAR}(z)$, at any given time, was larger for the cultures with smaller biomass concentration. In addition, for all three batches, the fluence rate after 96 h of cultivation was larger than the initial fluence rate despite the significantly larger biomass concentration (Fig. 1a). This was due to the decrease in the absorption cross-section (Fig. 2a) whose magnitude was significantly larger than the increase in biomass concentration. A similar increase in fluence rate as a function of time was experimentally observed by Pruvost et al. (2009) during nitrogen starvation cultivation of *Neochloris oleoabundans* in a flat-plate PBR. However, the fluence rate alone is not indicative of the amount of light absorbed by the cells (Pruvost and Cornet, 2012). Indeed, the absorption cross-section must also be considered as it accounts for the average amount of light absorbed by the cells. In fact, this is an important consideration during nitrogen starvation given the sharp decrease in absorption cross-section and the simultaneous increase in biomass concentration.

Fig. 3b shows the mean volumetric rate of energy absorption (MVREA) $\langle \mathscr{A} \rangle$, as a function of time for each sudden nitrogen starvation cultivation. It was estimated by Eqs. (1)–(3) using the corresponding experimentally measured average spectral mass absorption and scattering cross-sections $\bar{A}_{abs,\lambda}$ and $\bar{S}_{sca,\lambda}$. Here also, $\langle \mathscr{A} \rangle$ was larger for batches with smaller initial biomass concentration at all times. This could be attributed to the correspondingly larger fluence rate in the PBR (Fig. 3a). In addition, $\langle \mathscr{A} \rangle$ decreased with time for all three experiments. For example, in the sudden nitrogen starvation experiment with $X_0 = 0.23$ kg/m^3, $\langle \mathscr{A} \rangle$ was 24 $\mu mol_{hv}/g\ s$ initially but decreased to 6.6 and 5.4 $\mu mol_{hv}/g\ s$ after 72 and 96 h, respectively. This may seem counterintuitive since the fluence rate increased during nitrogen starvation (Fig. 3a). However, the decrease in the absorption cross-section dominated over the increase in the fluence rate. As previously suggested, MVREA $\langle \mathscr{A} \rangle$ is indicative of the amount of energy absorbed by the microalgae, unlike the fluence rate $G_{PAR}(z)$. The decrease in MVREA $\langle \mathscr{A} \rangle$ demonstrates that, on average, the energy absorbed per cell decreased during nitrogen starvation. This may negatively impact both cell division and lipid synthesis (Pruvost and Cornet, 2012).

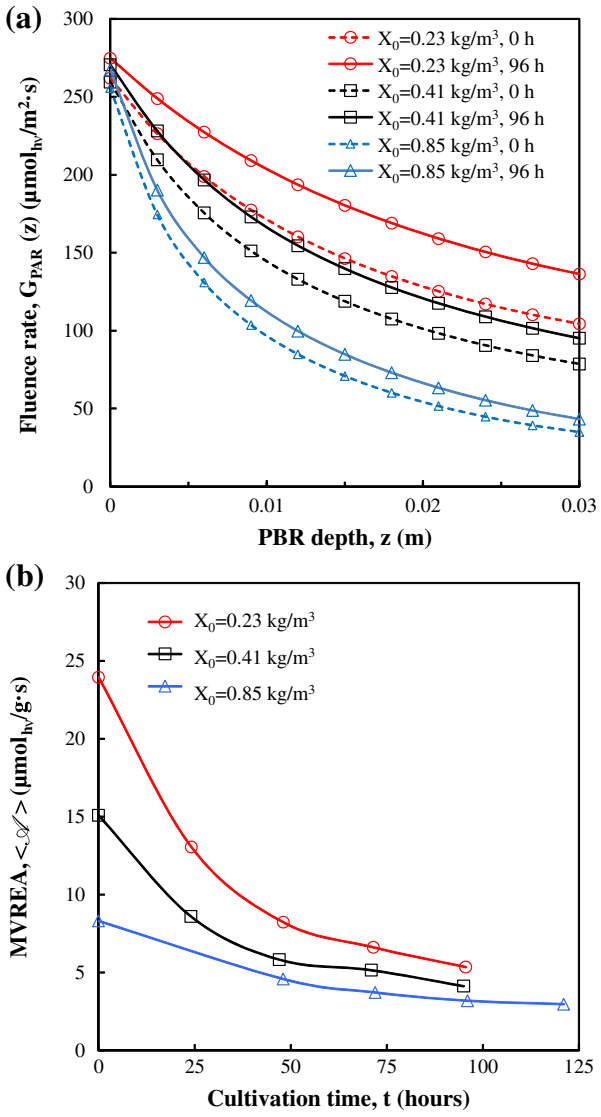

Fig. 3. (a) Fluence rate $G_{PAR}(z)$ in the PBR at the start of the cultivation (0 h) and after 96 h and (b) temporal evolution of MVREA $\langle \mathscr{A} \rangle$ for sudden starvation experiments with initial biomass concentration X_0 equal to 0.23, 0.41, and 0.85 kg/m^3.

Indeed, microalgae rely on the absorption of incident photons to carry out biochemical reactions. Their inability to absorb light could reduce their efficacy in performing photosynthesis and in fixating inorganic carbon (le B. Williams and Laurens, 2010).

4.7. TG-FA productivity

As previously discussed, cells synthesize TG-FA to store carbon and energy. Thus, the rate of TG-FA production should correlate with the mean volumetric rate of energy absorption (MVREA). The daily areal average productivity $\bar{R}(t_i)$ was estimated from experimental measurements at discrete time t_i according to Eq. (6). Similarly, the average daily MVREA was defined as $\overline{\langle \mathscr{A} \rangle}(t_i) = [\langle \mathscr{A} \rangle(t_i) + \langle \mathscr{A} \rangle(t_{i-1})]/2$ where $t_i - t_{i-1} = 24$ h. Fig. 4 shows the daily average areal TG-FA production rate $\bar{R}$ versus the daily average MVREA $\overline{\langle \mathscr{A} \rangle}$ for the sudden starvation experiments with three different initial concentrations X_0. For each experiment, the maximum daily productivity corresponded to the maximum MVREA $\overline{\langle \mathscr{A} \rangle}$ occurring on the first day of cultivation. Interestingly, data for the different experiments were consistent with one

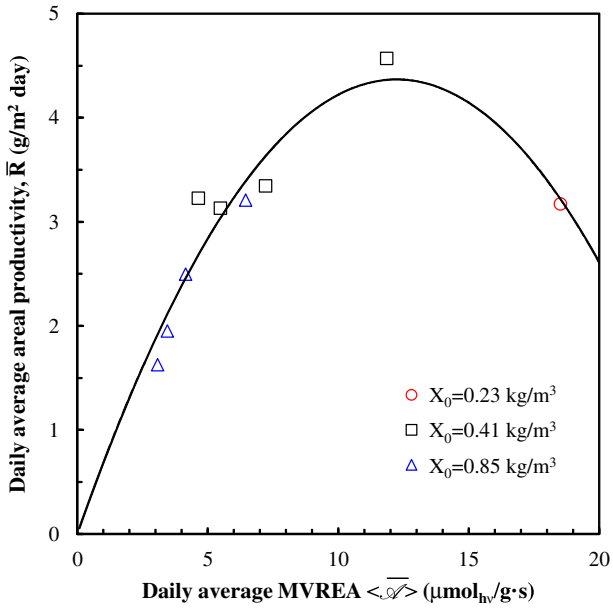

Fig. 4. Daily average areal TG-FA productivity $\bar{R}$ (in g/m^2 day) versus daily average MVREA $\langle\overline{\mathscr{A}}\rangle$ for sudden starvation experiments with incident PDF of 250 μmol$_{hv}$/m^2 s and initial biomass concentrations X_0 equal to 0.23, 0.41, and 0.85 kg/m^3.

another. A parabolic relationship between TG-FA productivity $\bar{R}$ and daily average MVREA $\langle\overline{\mathscr{A}}\rangle$ was fitted to the experimental data for convenience and for a lack of a better model. The peak productivity of 4.6 g/m^2 day was observed for MVREA equal to 13 μmol$_{hv}$/g s.

This relationship indicates that nitrogen starvation alone does not guarantee large TG-FA production rate. The TG-FA biosynthesis kinetics appears to be limited by the photon absorption rate represented by MVREA $\langle\overline{\mathscr{A}}\rangle$. This is analogous to microalgae grown under optimal growth conditions (i.e., without nutrient deprivation) when biomass productivity is only limited by light. Increasing MVREA per unit mass of microalgae can be achieved by reducing the biomass concentration. However, below a certain optimum value, the biomass productivity decreases and the light incident on the PBR is not fully absorbed (Takache et al., 2012; Pruvost and Cornet, 2012). In this so-called kinetic regime, biomass productivity is limited by the biosynthesis rate of the microalgae. Similarly, increasing the daily average MVREA beyond its optimal value resulted in a decrease in the daily TG-FA productivity $\bar{R}$. However, due to the reduction in pigment content and in absorption cross-section, it was not possible to achieve complete light absorption in the PBR during nitrogen starvation. Here, the process was biologically limited by the maximum TG-FA accumulation allowed in cells. For example, increasing daily average MVREA $\langle\overline{\mathscr{A}}\rangle$ on the first day of cultivation from 15 to 24 μmol$_{hv}$/g s was achieved by lowering the initial biomass concentration X_0 from 0.41 to 0.23 kg/m^3. Both experiments yielded cells with 31 dry wt.% TG-FA concentration after 24 h of cultivation. However, the corresponding TG-FA concentration in the PBR was 0.21 and 0.12 kg/m^3, respectively. Thus, increasing MVREA $\langle\overline{\mathscr{A}}\rangle$ did not affect the TG-FA concentration per cell but resulted in a smaller PBR daily TG-FA productivity due to the smaller biomass concentration.

Furthermore, there was a large difference in the temporal evolution of biomass concentration for experiments with initial biomass concentration X_0 of 0.41 and 0.85 kg/m^3 for the duration of the batch culture. By contrast, both experiments featured a similar TG-FA concentration after 24 and 48 h of cultivation. However, the daily TG-FA productivity of the PBR with $X_0 = 0.41$ kg/m^3 during the first 24 h of cultivation was much larger than that of the PBR with $X_0 = 0.85$ kg/m^3 due to its lower initial TG-FA concentration. On the other hand, between 24 and 48 h both experiments featured a similar TG-FA concentration and therefore a similar daily TG-FA productivity. It is interesting to note that they both featured similar values of daily average MVREA $\langle\overline{\mathscr{A}}\rangle$. This was illustrated in Fig. 4 for daily average MVREA $\langle\overline{\mathscr{A}}\rangle$ values of 5.5–7.5 μmol$_{hv}$/g s where data from both experiments were clustered. This exemplifies the value of our proposed method of correlating the MVREA with the TG-FA productivity. Despite the differing biomass and pigment concentrations, cultures with comparable values in MVREA featured similar TG-FA productivities.

Finally, During sudden starvation batch cultivations the TG-FA productivity $R(t)$ decreased due to the decrease in MVREA $\langle\mathscr{A}\rangle$ (Fig. 3b). Thus, in batch cultivation it is not possible to maintain a constant TG-FA productivity. Instead, the TG-FA productivity can be optimized through the initial value of MVREA denoted by $\langle\mathscr{A}_0\rangle$. The latter can be adjusted by changing the initial biomass concentration according to the incident PFD and PBR thickness.

4.8. TG-FA accumulation

Here, the data reported by Van Vooren et al. (2012) was used in addition to those reported in this study to elucidate the relationship between initial value of MVREA $\langle\mathscr{A}_0\rangle$ and TG-FA cell content. The authors performed a total of fourteen progressive and sudden starvation experiments using the same microalgae species, strain, and PBR as those used in the present study. The pigment and biomass concentrations were analyzed using the same protocols. In addition, the authors reported the pigment concentrations and the TG-FA concentrations in the cells for a wide range of nitrogen starvation experiments. However, they did not measure the radiation characteristics of *N. oculata*. Therefore, in order to extend the present light transfer analysis to experiments reported by Van Vooren et al. (2012), Eq. (19) was used to estimate the average mass absorption cross-section of cultures based on the reported pigment concentrations.

4.8.1. Sudden nitrogen starvation

Van Vooren et al. (2012) performed a total of four sudden starvation experiments in a PBR exposed to 250 μmol$_{hv}$/m^2 s. The initial biomass concentrations were 0.23, 0.41, 0.65, and 0.75 kg/m^3. The four experiments yielded cultures with a TG-FA concentration of 44, 45, 14, and 13 dry wt.%, after 96 h respectively. Fig. 5 shows the TG-FA cell content (in wt.%) after 96 h as a function of the initial MVREA $\langle\mathscr{A}_0\rangle$ for sudden starvation experiments performed in the present study and those reported by Van Vooren et al. (2012). It suggests that there exists a critical initial MVREA $\langle\mathscr{A}_0\rangle_{cr}$ beyond which the cells accumulated large amounts of TG-FA. Here, $\langle\mathscr{A}_0\rangle_{cr}$ was estimated to be 13 μmol$_{hv}$/g s. Note that it is generally not possible to exceed this critical initial MVREA $\langle\mathscr{A}_0\rangle_{cr}$ on the second day of sudden starvation cultivation. Indeed, a sharp decrease in $\langle\mathscr{A}\rangle$ was observed in the first 24 h of cultivation (Fig. 3b) due to the rapid decrease in pigment concentrations (Fig. 1b and c) and increase in biomass concentration. Therefore, in order to produce cells with large TG-FA content in a batch culture, the initial mass concentration X_0 of the batch culture must be adjusted carefully in order to achieve values of $\langle\mathscr{A}_0\rangle$ that exceed the critical MVREA $\langle\mathscr{A}_0\rangle_{cr} = 13$ μmol$_{hv}$/g s.

The critical MVREA under nitrogen starvation could correspond to conditions when the cells' TG-FA synthesis rate increases with respect to the synthesis rate of carbohydrate, protein, etc. In fact, the TG-FA synthesis pathway is activated under nitrogen starvation to act as an electron sink and prevent creation of excess free-radicals in the photosynthetic electron transport chain (Hu et al., 2008). In addition, it takes twice as much light energy to

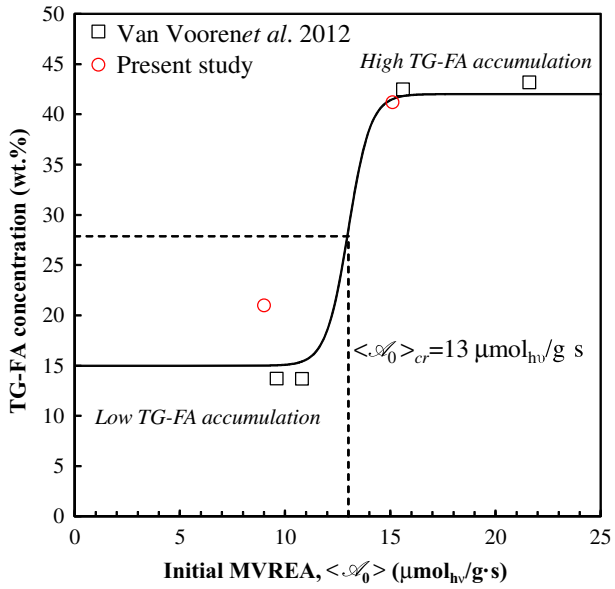

Fig. 5. TG-FA concentration (in wt.%) after 96 h of sudden nitrogen starvation as a function of initial MVREA $\langle \mathscr{A}_0 \rangle$. A critical value $\langle \mathscr{A}_0 \rangle_{cr}$ of 13 $\mu mol_{hv}/g\,s$ was necessary to trigger large TG-FA accumulation in cells.

produce TG-FA as it does to produce protein or carbohydrate of equal mass (Hu et al., 2008). However, it remains unclear how cells distribute the absorbed energy during nitrogen starvation (Hu et al., 2008). By setting the initial MVREA in excess of $\langle \mathscr{A}_0 \rangle_{cr}$ in batch experiments, the average MVREA was sufficient to ensure the average production rate of TG-FA was at least 40–45% of the biomass production rate for the duration of the experiment and produced cells with 40–45 dry wt.% TG-FA.

The similarity between the critical initial MVREA $\langle \mathscr{A}_0 \rangle_{cr}$ for maximum TG-FA cell content and the daily MVREA $\langle \overline{\mathscr{A}} \rangle$ corresponding to peak daily average areal productivity $\bar{R}$ is interesting but unsurprising. It can be explained by the fact that the largest increase in TG-FA concentration in cells and maximum daily productivity for each cultivation occurred in the first 24 h of nitrogen starvation. Since, the daily average MVREA $\langle \overline{\mathscr{A}} \rangle$ for the first 24 h of cultivation corresponded approximately to the initial MVREA $\langle \mathscr{A}_0 \rangle$, the optimum values for both were equal.

4.8.2. Progressive starvation

Van Vooren et al. (2012) performed a total of 10 progressive starvation experiments as summarized in Table 2 of their manuscript. Experiments No. 9 and 10 used a modified Conway medium with an initial NO_3^- concentration of 0.92 and 1.65 mM, respectively. In both cases, the initial biomass concentration was 0.02 kg/m^3 and the microorganisms were cultivated in a 150 L PBR, 5 cm in thickness, exposed to a PFD of 222 $\mu mol_{hv}/m^2\,s$. Note that the biomass concentration at the culture's onset of nitrogen starvation was not reported in experiments No. 1 to 8. Therefore, it was not possible to estimate the radiation characteristics and the MVREA $\langle \mathscr{A} \rangle$ for those experiments.

Fig. 6a and b respectively present the temporal evolution of the MVREA $\langle \mathscr{A} \rangle$ and of the cellular TG-FA concentration during the course of experiments No. 9 and 10. The approximate time at which nitrogen starvation began was estimated from elemental analysis assuming that *N. oculata* was composed of 10 dry wt.% nitrogen in nutrient replete conditions (Takache et al., 2012). Nitrogen starvation occured later in experiment No. 10 than in experiment No. 9 because of the larger initial nitrate concentration. For both experiments, the extrapolated MVREA $\langle \mathscr{A}_0 \rangle$ at the onset of

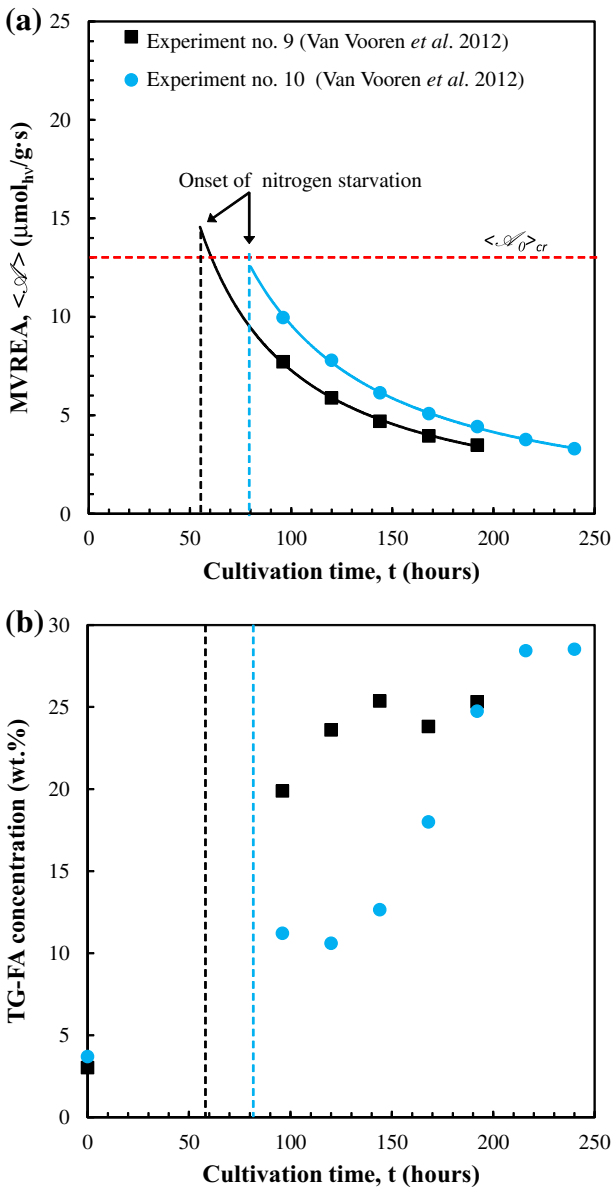

Fig. 6. Temporal evolution of (a) MVREA $\langle \mathscr{A} \rangle$ and (b) cellular TG-FA concentration for progressive starvation batch cultures grown in a 150 L PBR, 5 cm in thickness, in modified Conway medium with an initial NO_3^- concentration of 0.93 mM (experiment No. 9) and 1.65 mM (experiment No. 10) by Van Vooren et al. (2012). The dashed lines indicate the estimated time at which nitrogen starvation began.

the nitrogen starvation fell between 12 and 15 $\mu mol_{hv}/g\,s$. This corresponded, approximately, to the value of the critical MVREA $\langle \mathscr{A}_0 \rangle_{cr}$ observed in the sudden starvation experiments. The intracellular TG-FA concentration increased sharply after nitrogen starvation began and reached 28 dry wt.%. It is remarkable that both progressive and sudden starvation experiments had a similar MVREA at the onset of nitrogen starvation since it is not possible to control and set MVREA at the onset of nitrogen starvation $\langle \mathscr{A}_0 \rangle$ for progressive nitrogen starvation experiments. This provided further evidence in the relevance of MVREA $\langle \mathscr{A}_0 \rangle$ in predicting the TG-FA accumulation in cells.

Along with nitrogen starvation, the term "light stress" has often been used in the literature as a necessary condition for large TG-FA productivity (Hu et al., 2008). However, the concept of "light stress" has remained qualitative. The present study addressed this issue by defining the physical variable to quantify "light stress",

namely the specific volumetric rate of energy absorption (MVREA). It also reported the critical value of the MVREA necessary for large TG-FA productivity.

The maximum batch averaged areal TG-FA and biomass productivities achieved were respectively 2.9 and 7.5 g/m^2 day, obtained for the experiment with initial biomass concentration $X_0 = 0.41$ kg/m^3. The associated volumetric TG-FA and biomass productivities were 0.1 and 0.25 kg/m^3 day, respectively. These productivities could be significantly increased by optimizing the MVREA in the PBR using the proposed relation between TG-FA productivity R and MVREA $\langle \mathscr{A} \rangle$. The latter can also be used to predict the TG-FA productivity of PBRs of all scales and optimize them as long as rigorous radiation transfer analysis is performed to estimate MVREA $\langle \mathscr{A} \rangle$. Pruvost and Cornet (2012) validated this approach by optimizing and predicting both biomass concentration and productivity of microorganisms in PBRs scaling from 1 to 150 L.

Future studies should focus on validating the present observations and quantitative analysis for other microalgae species and developing novel methods of optimizing the instantaneous TG-FA production rate R with respect to MVREA $\langle \mathscr{A} \rangle$. The latter depends on biomass concentration, cell pigment content, and incident PFD. These parameters are dynamic and interdependent. They will be difficult to control, especially in a batch cultivation exposed to solar radiation. Therefore, while an optimum value of MVREA exists that maximizes TG-FA productivity, it may not be trivial to control and optimize MVREA $\langle \mathscr{A} \rangle$. Moreover, the optimum and critical MVREA may depend on culture conditions such as medium salinity, pH, or temperature. In the present study, the microalgae were cultivated under conditions leading to maximal biomass and TG-FA productivity reported by Van Vooren et al. (2012) and Pruvost et al., 2009. The methodology presented here could be extended to investigate the effects of cultivation conditions on the optimal and critical MVREA.

5. Conclusion

This study demonstrated the existence of a relation between the mean volumetric rate of energy absorption (MVREA) per unit mass of microalgae and the daily TG-FA productivity of *N. oculata* cultures. It indicated that TG-FA synthesis in the PBR was physically limited by the photon absorption rate per unit mass of microalgae. The TG-FA productivity reached a maximum of 4.5 g/m^2 day corresponding to MVREA equal to 13 μmol_{hv}/g s. In addition, a critical initial MVREA $\langle \mathscr{A}_0 \rangle_{cr}$ in excess of also 13 μmol_{hv}/g s was required to trigger a large accumulation of TG-FA in cells in both sudden and progressive nitrogen starvation.

Acknowledgments

This research was supported by the US National Science Foundation through IGERT program on Clean Energy for Green Industry at UCLA (DGE-0903720) and the French National Research Agency project DIESALG (ANR-12-BIME-0001-02). R.K. is grateful to the Embassy of France in the United States, Office for Science and Technology for the Chateaubriand Fellowship.

Appendix A. Supplementary data

Supplementary data associated with this article can be found, in the online version, at http://dx.doi.org/10.1016/j.biortech.2014.04.045.

References

Adams, C., Godfrey, V., Wahlen, B., Seefeldt, L., Bugbee, B., 2013. Understanding precision nitrogen stress to optimize the growth and lipid content tradeoff in oleaginous green microalgae. Bioresource Technology 131 (1), 188–194.

Berberoğlu, H., Yin, J., Pilon, L., 2007. Light transfer in bubble sparged photobioreactors for H_2 production and CO_2 mitigation. International Journal of Hydrogen Energy 32 (13), 2273–2285.

Berberoğlu, H., Pilon, L., Melis, A., 2008. Radiation characteristics of *Chlamydomonas reinhardtii* CC125 and its truncated chlorophyll antenna transformants *tla1*, *tlaX* and *tla1-CW+*. International Journal of Hydrogen Energy 33 (22), 6467–6483.

Berges, J., Franklin, D., Harrison, P., 2001. Evolution of an artificial seawater medium: Improvements in enriched seawater, artificial water over the last two decades. Journal of Phycology 37 (6), 1138–1145.

Bidigare, R.R., Ondrusek, M.E.E., Morrow, J.H.H., Kiefer, D.A.A., 1990. In-vivo absorption properties of algal pigments. Proceedings of the SPIE 1302, 290–302.

Bissett, W., Patch, J., Carder, K., Lee, Z., 1997. Pigment packaging and chlorophyll *a*-specific absorption in high-light oceanic waters. Limnology and Oceanography 42 (5), 961–968.

Breuer, G., Lamers, P.P., Martens, D., Draaisma, R., Wijffels, R., 2013. Effect of light intensity, pH, and temperature on triacylglycerol (TAG) accumulation induced by nitrogen starvation in *Scenedesmus obliquus*. Bioresource Technology 143, 1–9.

Bricaud, A., Claustre, H., Ras, J., Oubelkheir, K., 2004. Natural variability of phytoplanktonic absorption in oceanic waters: Influence of the size structure of algal populations. Journal of Geophysical Research 109 (C11), 1947–1960.

Cassano, A., Martin, C., Brandi, R., Alfano, O., 1995. Photoreactor analysis and design: Fundamentals and applications. Industrial & Engineering Chemistry Research 34 (7), 2155–2201.

Chisti, Y., 2007. Biodiesel from microalgae. Biotechnology Advances 25 (3), 294–306.

Cohen, Z., 1999. Chemicals from Microalgae. Taylor & Francis, London, UK.

Cornet, J.-F., Dussap, C.-G., 2009. A simple and reliable formula for assessment of maximum volumetric productivities in photobioreactors. Biotechnology Progress 25 (2), 424–435.

Dauchet, J., Blanco, S., Cornet, J., Hafi, M.E., Eymet, V., Fournier, R., 2013. The practice of recent radiative transfer Monte Carlo advances and its contribution to the field of microorganisms cultivation in photobioreactors. Journal of Quantitative Spectroscopy and Radiative Transfer 128, 52–59.

Flynn, K., Davidson, K., Cunningham, A., 1993. Relations between carbon and nitrogen during growth of *Nannochloropsis oculata* (droop) Hibberd under continuous illumination. New Phytologist 125 (4), 717–722.

Heath, M., Richardson, K., Kirboe, T., 1990. Optical assessment of phytoplankton nutrient depletion. Journal of Plankton Research 12 (2), 381–396.

Hu, Q., Sommerfeld, M., Jarvis, E., Ghirardi, M., Posewitz, M., Seibert, M., Darzins, A., 2008. Microalgal triacylglycerols as feedstocks for biofuel production: perspectives and advances. The Plant Journal 54 (4), 621–639.

Jonasz, M., Fournier, G., 2007. Light Scattering by Particles in Water: Theoretical and Experimental Foundations. Academic Press, San Diego, CA.

Kandilian, R., Lee, E., Pilon, L., 2013. Radiation and optical properties of *Nannochloropsis oculata* grown under different irradiances and spectra. Bioresource Technology 137, 63–73.

Ke, B., 2001. Photosynthesis: Photobiochemistry and Photobiophysics. Advances in Photosynthesis. Kluwer Academic Publishers, Dordrecht, The Netherlands.

le B. Williams, P.J., Laurens, L., 2010. Microalgae as biodiesel and biomass feedstocks: Review and analysis of the biochemistry, energetics and economics. Energy and Environmental Science 3, 554–590.

Lee, E., Pruvost, J., He, X., Munipalli, R., Pilon, L., 2014. Design tool and guidelines for outdoor photobioreactors. Chemical Engineering Science 116, 18–29.

Nelson, N., Prezelinl, B., Bidigare, R., 1993. Phytoplankton light absorption and the package effect in California coastal waters. Marine Ecology Progress Series 94, 217–227.

Oeschger, L., Posten, C., 2012. Construction and assessment parameters of photobioreactors. In: Posten, C., Walter, C. (Eds.), Microalgal Biotechnology: Potential and Production. De Gruyter, Berlin, Germany, pp. 225–236.

Pal, D., Khozin-Goldberg, I., Cohen, Z., Boussiba, S., 2011. The effect of light, salinity, and nitrogen availability on lipid production by *Nannochloropsis* sp. Applied Microbiology and Biotechnology 90 (4), 1429–1441.

Pilon, L., Berberoğlu, H., Kandilian, R., 2011. Radiation transfer in photobiological carbon dioxide fixation and fuel production by microalgae. Journal of Quantitative Spectroscopy and Radiative Transfer 112 (17), 2639–2660.

Pottier, L., Pruvost, J., Deremetz, J., Cornet, J., Legrand, J., Dussap, C., 2005. A fully predictive model for one-dimensional light attenuation by Chlamydomonas reinhardtii in a torus photobioreactor. Biotechnology and Bioengineering 91 (5), 569–582.

Pruvost, J., Cornet, J., 2012. Knowledge models for the engineering and optimization of photobioreactors. In: Posten, C., Walter, C. (Eds.), Microalgal Biotechnology: Potential and Production. De Gruyter, Berlin, Germany, pp. 181–224.

Pruvost, J., Vooren, G.V., Cogne, G., Legrand, J., 2009. Investigation of biomass and lipids production with Neochloris oleoabundans in photobioreactor. Bioresource Technology 100 (23), 5988–5995.

Ritchie, R., 2006. Consistent sets of spectrophotometric chlorophyll equations for acetone, methanol and ethanol solvents. Photosynthesis Research 89 (1), 27–41.

Strickland, J., Parsons, T., 1968. A Practical Handbook of Seawater Analysis: Pigment Analysis. Bulletin of Fisheries Research Board of Canada. Fisheries Research Board of Canada.

Takache, H., Christophe, G., Cornet, J.-F., Pruvost, J., 2010. Experimental and theoretical assessment of maximum productivities for the microalgae Chlamydomonas reinhardtii in two different geometries of photobioreactors. Biotechnology Progress 26 (2), 431–440.

Takache, H., Pruvost, J., Cornet, J.-F., 2012. Kinetic modeling of the photosynthetic growth of Chlamydomonas reinhardtii in a photobioreactor. Biotechnology Progress 28 (3), 681–692.

Van Vooren, G., Grand, F.L., Legrand, J., Cuine, S., Peltier, G., Pruvost, J., 2012. Investigation of fatty acids accumulation in Nannochloropsis oculata for biodiesel application. Bioresource Technology 124, 421–432.